

Impact of QCD corrections on the search for the intermediate mass Higgs boson

B. Bailey

Department of Physics, B-159, Florida State University, Tallahassee, Florida 32306

D. Graudenz

*Theoretical Physics Group, Lawrence Berkeley Laboratory, University of California,
1 Cyclotron Road, Berkeley, California 94720*

(Received 23 July 1993)

Using next-to-leading-log calculations of Higgs boson production and hadronic two-photon production, a signal and background study in the intermediate mass range of the Higgs boson is done for $\sqrt{s} = 40$ and 14 TeV. The effects of realistic cuts, including photon isolation, are examined.

PACS number(s): 12.38.Bx, 14.70.Hp, 14.80.Bn

I. INTRODUCTION

The Higgs boson and the top quark are the remaining missing pieces of the standard model. The top quark, if its mass is less than 250 GeV, is expected to be discovered at the Fermilab Tevatron [1] and CERN e^+e^- collider LEP has set a lower bound on the Higgs boson mass of $m_H > 57$ GeV [2]. LEP II, with a center-of-mass energy of 180 GeV, will be able to extend the search to 90 GeV [3]. If $m_H > 90$ GeV, high-energy colliders such as the Superconducting Super Collider (SSC) and/or CERN Large Hadron Collider (LHC) will be required to extend the search.

The dominant production mechanism at hadron supercolliders is expected to be $gg \rightarrow H$ [4]. The dominant decay mode depends on the Higgs boson mass. If m_H is greater than twice the Z mass the four-lepton decay mode, $H \rightarrow ZZ \rightarrow 4l$, should be observable [4]. If the Higgs mass lies in the "intermediate mass region," $80 \text{ GeV} < m_H < 2M_Z$, QCD backgrounds overwhelm the main decay mode $H \rightarrow b\bar{b}$ and the rare processes $H \rightarrow ZZ^*$ and $H \rightarrow \gamma\gamma$ become the decay modes of choice [5]. The decay $H \rightarrow ZZ^*$ occurs at observable rates for $m_H > 130$ GeV and $H \rightarrow \gamma\gamma$ occurs at observable rates for the entire intermediate mass region. Unfortunately, the two-photon decay mode is plagued by a large background [6] and detection of the inclusive process $pp \rightarrow H \rightarrow \gamma\gamma$ will require detectors with excellent $\gamma\gamma$ mass resolution [7].

Alternative production mechanisms which eliminate the large two-photon background by the inclusion of a final state lepton have been studied [8–11]. These production mechanisms include associated $W H$, or $t\bar{t} H$ production with $H \rightarrow \gamma\gamma$. Including cuts, the expected number of such events per year at the SSC (LHC), assuming $\sqrt{s} = 40$ (14) TeV and a luminosity of 10 fb^{-1} , is ~ 20 (4). By comparison, for $m_H = 140$ GeV the expected number of $pp \rightarrow H \rightarrow \gamma\gamma$ events per year is ~ 700 (300) at the SSC (LHC). The Higgs boson can be discovered via the $l\gamma\gamma$ signal but confirmation of the discovery in the $\gamma\gamma$ channel would provide a margin of certainty. Clearly the $\gamma\gamma$ channel requires precise knowledge of the

two-photon signal and background.

Recently, next-to-leading-log (NLL) calculations of Higgs production [12–14] and photon pair production have been performed [15, 16]. The photon pair production calculation was performed in a Monte Carlo environment. The flexibility of the Monte Carlo calculation allows a thorough study of the effect of various kinematic and isolation cuts on the two-photon background. In order to make useful comparisons between signal and background, the signal $pp \rightarrow H \rightarrow \gamma\gamma$ was recalculated using the NLL Monte Carlo formalism. In this paper the effect of kinematic and isolation cuts on the signal and background is examined at the NLL level (for the intermediate mass region). Results are presented for both the SSC and LHC.

The rest of this paper is organized as follows. In Sec. II, details of the calculation as well as input parameters are discussed. In Sec. III, numerical results are presented. In Sec. IV, the impact of further QCD corrections are discussed. In Sec. V, a brief summary and conclusions are presented.

II. CALCULATION

The Monte Carlo formalism for next-to-leading-log (NLL) calculations has been described in detail in Refs. [15–17]. The explicit details for the two-photon calculation can be found in Ref. [15] and will not be repeated here. The NLL Monte Carlo calculation of the signal $pp \rightarrow H$ proceeds in a similar manner.

The leading-log (LL) signal consists of the Born process ($pp \rightarrow H$) followed by the decay $H \rightarrow \gamma\gamma$. The Higgs decay is calculated in the Higgs center-of-mass frame and then boosted into the hadron-hadron center-of-mass frame. The Higgs branching fractions are calculated as per Ref. [4]. Including the order- α_s corrections to the Born process we obtain the NLL signal. The matrix element is calculated in the approximation of a top quark with infinite mass. The "K-factor," NLL/LL, in this limit is then multiplied by the Born term for a finite top quark mass. This procedure yields an excellent approx-

imation to the general case, even for top quark masses above threshold [14].

The two-photon background consists of several contributions: Born, gluon box, single- and double-photon fragmentation processes, and the order- α_s corrections to the Born process. The gluon box is an order- $\alpha^2\alpha_s^2$ process but due to the large gluon luminosity it cannot be neglected. For the remainder of this paper the leading-log background contribution will be defined as LL = Born + box + single fragmentation + double fragmentation and NLL = LL + order- α_s corrections to the Born process.

Unless otherwise stated the following are used for this calculation: CTEQ Collaboration set 1M (CTEQ1M) parton distributions [18], the two-loop expression for $\alpha_s(Q^2)$, $Q^2 = p_{T\gamma}^2$, and $m_t = 140$ GeV. Additionally, for the SSC, the following cuts utilized in studies by the Gamma-E-Mu Collaboration and Solenoidal Detector Collaboration (GEM) and (SDC) [7] are used: $p_{T\gamma} > 20$ GeV, $|y_\gamma| < 2.5$, $|\cos\theta^*| < 0.7$, isolation cone $R \equiv \sqrt{\Delta y^2 + \Delta\phi^2} = 0.7$, and hadronic energy inside of isolation cone < 4 GeV. For the LHC, the following ATLAS [19] inspired cuts are used: $p_{T\gamma}^1 > 30$ GeV, $p_{T\gamma}^2 > 20$ GeV, $|y_\gamma| < 2.5$, isolation cone $R \equiv \sqrt{\Delta y^2 + \Delta\phi^2} = 0.255$, $p_{T\gamma}^1/(p_{T\gamma}^1 + p_{T\gamma}^2) < 0.7$, and hadronic energy inside of isolation cone < 5 GeV.

III. RESULTS

Defining a K factor as $K = \text{NLL}/\text{LL}$, Fig. 1 shows the variation of this correction factor with photon-pair mass (i.e., Higgs mass) for the SSC (using GEM and/or SDC cuts). The solid curve denotes the variation for the signal and the dashed curve for the background. Specific values for the signal and the background may be found in Tables I and II.

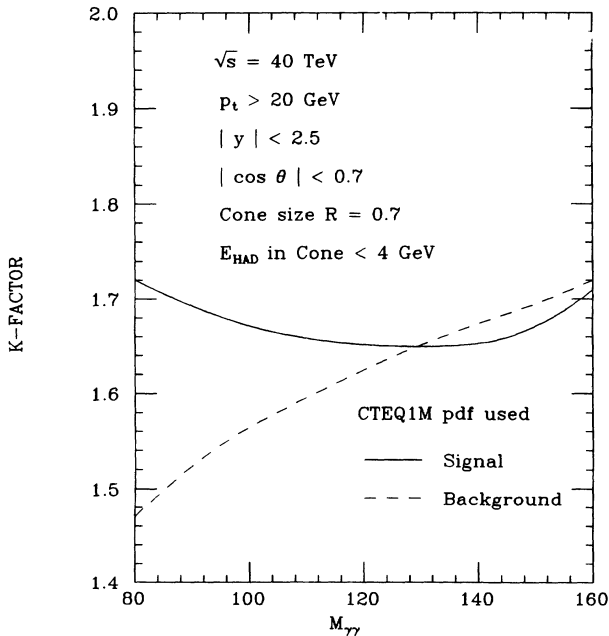


FIG. 1. K factor for the signal and background at $\sqrt{s} = 40$ TeV using GEM and/or SDC cuts.

TABLE I. Signal (fb) at $\sqrt{s} = 40$ TeV with GEM and/or SDC cuts.

m_H	$\sigma_{\text{LL}}(pp \rightarrow H \rightarrow \gamma\gamma)$	$\sigma_{\text{NLL}}(pp \rightarrow H \rightarrow \gamma\gamma)$	K factor
80	39	67	1.72
90	49	82	1.67
100	59	100	1.69
110	70	117	1.67
120	76	125	1.64
130	72	117	1.63
140	57	93	1.63
150	37	60	1.62
160	7	12	1.71

TABLE II. Background (fb/GeV) at $\sqrt{s} = 40$ TeV with GEM and/or SDC cuts.

m_H	$\frac{d\sigma_{\text{LL}}(pp \rightarrow H \rightarrow \gamma\gamma)}{dM_{\gamma\gamma}}$	$\frac{d\sigma_{\text{NLL}}(pp \rightarrow \gamma\gamma)}{dM_{\gamma\gamma}}$	K factor
80	761	1121	1.47
90	496	780	1.57
100	340	522	1.54
110	237	377	1.59
120	173	283	1.64
130	128	212	1.66
140	98	163	1.66
150	75	127	1.69
160	60	103	1.72

TABLE III. Signal (fb) at $\sqrt{s} = 14$ TeV with ATLAS type cuts.

m_H	$\sigma_{\text{LL}}(pp \rightarrow H \rightarrow \gamma\gamma)$	$\sigma_{\text{NLL}}(pp \rightarrow H \rightarrow \gamma\gamma)$	K factor
80	13.7	35.3	2.58
90	18.3	44.5	2.43
100	22.9	53.5	2.34
110	27.1	61.2	2.26
120	29.2	64.9	2.22
130	27.4	59.4	2.17
140	21.6	46.1	2.13
150	13.8	29.1	2.11
160	2.62	5.43	2.07

TABLE IV. Background (fb/GeV) at $\sqrt{s} = 14$ TeV with ATLAS type cuts.

m_H	$\frac{d\sigma_{\text{LL}}(pp \rightarrow H \rightarrow \gamma\gamma)}{dM_{\gamma\gamma}}$	$\frac{d\sigma_{\text{NLL}}(pp \rightarrow \gamma\gamma)}{dM_{\gamma\gamma}}$	K factor
80	328	667	2.03
90	249	501	2.01
100	188	372	1.98
110	142	286	2.01
120	108	210	1.94
130	84	162	1.93
140	66	127	1.92
150	53	101	1.91
160	42	79	1.88

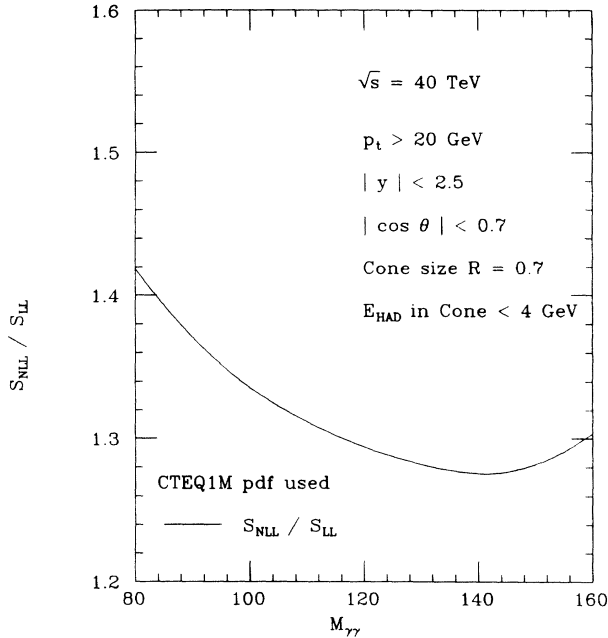


FIG. 2. Ratio NLL significance to LL significance at $\sqrt{s} = 40$ TeV using GEM and/or SDC cuts.

Figure 1 shows that the situation for a light Higgs boson ($80 \text{ GeV} < m_H < 100 \text{ GeV}$) may be better than previously assumed. In this region the K factor for the background is decreasing while the K factor for the signal is increasing for decreasing Higgs mass. The effect of this behavior on the significance of the signal can be seen in Fig. 2. Figure 2 shows the ratio of QCD corrected significance to the leading-log significance. For the light mass region this curve implies that the discovery time may be reduced by up to a factor of 1.4, and for the rest

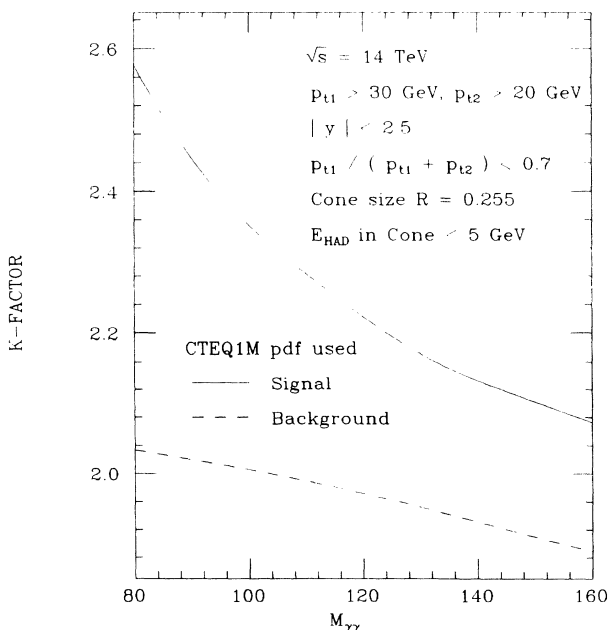


FIG. 3. K factor for the signal and background at $\sqrt{s} = 14$ TeV using ATLAS type cuts.

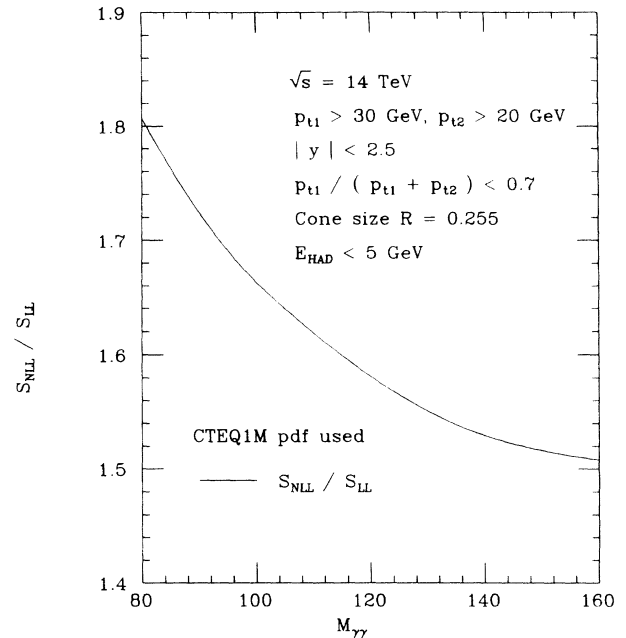


FIG. 4. Ratio NLL significance to LL significance at $\sqrt{s} = 14$ TeV using ATLAS type cuts.

of the mass region by a factor ~ 1.3 .

For the LHC, Fig. 3 shows the variation of the K factor with photon-pair mass (using ATLAS style cuts). As before, the solid curve denotes the variation for the signal and the dashed curve for the background. Specific values for the signal and the background may be found in Tables III and IV.

Figure 3 shows that the signal K factor dominates the background K factor over the entire mass range. The impact of this behavior on the significance of the signal can be seen in Fig. 4. Figure 4 shows the ratio of QCD corrected significance to the leading-log significance. For the light mass region this curve implies that the discovery time may be reduced by up to a factor of 1.8, and for the rest of the mass region by a factor ~ 1.5 .

IV. IMPACT OF ADDITIONAL QCD CORRECTIONS

A valid criticism of the results presented above would be the exclusion of QCD corrections to the background process $gg \rightarrow \gamma\gamma$. The QCD corrections to this process are unknown. This raises the following question: if the corrections to this process were similar in magnitude to the $gg \rightarrow H$ case how would this affect the results presented above?

At leading-log level the gluon box contributes $\sim 45\%$ (35%) to the background cross section at the SSC (LHC). At next-to-leading-log level, as presented above, this contribution drops to $\sim 25\%$ (18%) of the background due to the large corrections to the $q\bar{q} \rightarrow \gamma\gamma$ process. If the QCD K factor for the gluon box process is set equal to the K factor for $gg \rightarrow H$, the NLL background K factor is increased by a factor of 1.4 (1.2) at the SSC (LHC).

The net effect on the significance ratios shown in Figs. 2 and 4 is to reduce them by 15% for the SSC and by 9% for the LHC.

Another possible concern of the results presented above would be the exclusion of QCD corrections to the photon fragmentation processes. The fragmentation processes contribute significantly to the nonisolated LL cross section [6, 16] but $< 10\%$ of the isolated leading-log cross section.

The QCD corrections for photon fragmentation have recently been presented by Aurenche *et al.* in Ref. [20]. The results for NLL photon fragmentation fall below the LL curves for all values of z and converge for high z (z is the fraction of momentum the photon takes from its parent parton). For isolated photons the high z region is the relevant region that contributes to the cross section. Thus using the LL fragmentation results in a slight overestimate the fragmentation contribution and the impact on the results presented above is negligible.

V. CONCLUSIONS

Results have been presented, at the NLL level, for the signal and background in the intermediate mass region. The K factors, and the significance of the signal, were found to depend on the mass of the Higgs boson and the cuts implemented. The QCD corrections were found to imply that the discovery time for the intermediate mass Higgs boson could be reduced by a factor of 1.3–1.8 with the caveat that QCD corrections to the background process $gg \rightarrow \gamma\gamma$ could reduce these factors by 9–15%.

ACKNOWLEDGMENTS

This research was supported in part by the U.S. Department of Energy under Contract Nos. DE-FG05-87ER40319 and DE-AC03-76SF00098. The authors would like to thank I. Hinchliffe, J. Womersley, and R. Zhu for useful discussions. D.G. acknowledges support by the Max Kade Foundation, New York.

-
- [1] R. K. Ellis, *Phys. Lett. B* **259**, 492 (1991).
 - [2] S. L. Wu, in *The Vancouver Meeting—Particles and Fields '91*, Proceedings of the Joint Meeting of the Division of Particles and Fields of the American Physical Society and the Particle Physics Division of the Canadian Association of Physicists, Vancouver, 1991, edited by D. Axen, D. Bryman, and M. Comyn (World Scientific, Singapore, 1992).
 - [3] J. Gunion and L. Roszkowski, in *Research Directions for the Decade*, Proceedings of the Summer Study, Snowmass, Colorado, 1990, edited by E. Berger (World Scientific, Singapore, 1991); V. Barger and K. Whisnant, *Phys. Rev. D* **43**, 1443 (1991).
 - [4] J. Gunion, H. Haber, G. Kane, and S. Dawson, *The Higgs Hunter's Guide* (Addison-Wesley, Redwood City, CA, 1990).
 - [5] J. Gunion, G. Kane, and J. Wudka, *Nucl. Phys. B* **299**, 231 (1988).
 - [6] H. Baer and J. F. Owens, *Phys. Lett. B* **205**, 377 (1988).
 - [7] GEM Technical Design Report No. SSCL-SR-1219, 1993 (unpublished); SDC Technical Design Report No. SSCL-SR-1215, 1992 (unpublished).
 - [8] R. Kleiss, Z. Kunszt, and J. Stirling, *Phys. Lett. B* **253**, 269 (1991).
 - [9] W. Marciano and F. Paige, *Phys. Rev. Lett.* **66**, 2433 (1991); J. Gunion, *Phys. Lett. B* **261**, 510 (1991).
 - [10] T. Han and S. Willenbrock, *Phys. Lett. B* **273**, 167 (1990).
 - [11] H. Baer, B. Bailey, and J. F. Owens, *Phys. Rev. D* **47**, 2730 (1993).
 - [12] S. Dawson, *Nucl. Phys. B* **359**, 283 (1991).
 - [13] A. Djouadi, M. Spira, and P. M. Zerwas, *Phys. Lett. B* **264**, 440 (1991).
 - [14] D. Graudenz, M. Spira, and P. M. Zerwas, *Phys. Rev. Lett.* **70**, 1372 (1993).
 - [15] B. Bailey, J. Ohnemus, and J. F. Owens, *Phys. Rev. D* **46**, 2018 (1992).
 - [16] B. Bailey and J. F. Owens, *Phys. Rev. D* **47**, 2735 (1993).
 - [17] B. Bailey, Ph.D. dissertation, Florida State University, 1993; H. Baer and M. H. Reno, *Phys. Rev. D* **43**, 2892 (1991); J. Ohnemus and J. F. Owens, *ibid.* **43**, 3626 (1991); J. Ohnemus, *ibid.* **44**, 1403 (1991); **44**, 3477 (1991); H. Baer, J. Ohnemus, and J. F. Owens, *ibid.* **42**, 61 (1990); *Phys. Lett. B* **234**, 127 (1990); H. Baer, J. Ohnemus, and J. F. Owens, *Phys. Rev. D* **40**, 2844 (1989); L. Bergmann, Ph.D. dissertation, Florida State University, 1989.
 - [18] J. Botts, J. Morfin, J. F. Owens, J. W. Qiu, W. K. Tung, and H. Weerts, *Phys. Lett. B* **304**, 159 (1993).
 - [19] ATLAS letter of intent, Report No. CERN/LHCC/92-4, 1992 (unpublished).
 - [20] P. Aurenche, P. Chiappetta, M. Fontannaz, J. Ph. Guillet, and E. Pilon, *Nucl. Phys. B* **399**, 34 (1993).